photonics

MDPI

Communication

Bound States in the Continuum versus Fano Resonances: Topological Argument

Denis V. Novitsky [1,2,*] and Andrey V. Novitsky [2,3]

[1] Nanophotonics Center, B. I. Stepanov Institute of Physics, National Academy of Sciences of Belarus, Nezavisimosti Avenue 68, 220072 Minsk, Belarus
[2] Physics Faculty, Belarusian State University, Nezavisimosti Avenue 4, 220030 Minsk, Belarus
[3] Department of Physics and Engineering, ITMO University, Kronverksky Prospekt 49, 197101 St. Petersburg, Russia
* Correspondence: d.novitsky@ifanbel.bas-net.by

Abstract: There is a recent surge of interest to the bound states in the continuum (BICs) due to their ability to provide high-quality resonances in open photonic systems. They are usually observed in perturbed systems possessing Fano resonances in their spectra. We argue that, generally speaking, the Fano resonances should not be considered as a proxy for BICs (as it is often done) due to their fundamentally different topological properties. This difference is illustrated with the non-Hermitian layered structure supporting both topologically nontrivial quasi-BIC and topologically trivial Fano resonances. Non-Hermiticity can also be a source of additional topological features of these resonant responses. Moreover, the lasing mode associated with BIC in this structure also possesses nonzero topological charge that can be useful for producing unconventional states of light. This paper contributes to the discussion of BIC physics and raises new questions concerning topological properties of non-Hermitian systems.

Keywords: bound state in the continuum; Fano resonance; winding number; layered structure; non-Hermitian photonics

Citation: Novitsky, D.V.; Novitsky, A.V. Bound States in the Continuum versus Fano Resonances: Topological Argument. *Photonics* **2022**, *9*, 880. https://doi.org/10.3390/photonics9110880

Received: 17 October 2022
Accepted: 17 November 2022
Published: 20 November 2022

1. Introduction

Among anomalous features of light-matter interaction [1], the so-called bound states in the continuum (BICs) have attracted much attention recently. Known for many years in the context of quantum mechanics [2–4], they turned out to be in the spotlight of photonics research in the last decade. The reason is the exceptional properties of photonic BICs which are the non-radiative modes of open systems (cavities, metasurfaces, etc.). The perfect BIC can be treated as an infinitely narrow resonance having perfect radiation localization and infinite quality (Q) factor. There are two most general mechanisms of BIC formation—the symmetry protected BICs due to the symmetry mismatch between the modes supported by the structure and the continuum modes and the BICs via destructively interfering resonances (Friedrich-Wintgen BICs). These mechanisms are general enough to provide a wide variety of systems supporting BICs: from single particles to their arrays, metasurfaces and photonic crystals. Not pretending to discuss all the richness of BIC studies, we refer the reader to several recent review papers [5–8].

The strict BIC is a mathematical object and is unobservable in practice. Therefore, researchers deal with the quasi-BICs—finite-width resonances appearing under some perturbing conditions. The standard approach to transforming BIC into quasi-BIC is through violation of symmetry of the structure as impressively shown for metasurfaces [9,10]. For a single dielectric particle, quasi-BIC appears as a result of the deviation from the destructive interference of the Fabry-Perot and Mie resonances [11]. In any case, it is usually assumed that the Fano resonance appearing in the response of the perturbed system plays the role of the quasi-BIC [6]. Another point of view was presented

in Ref. [12] where the quasi-BIC associated with the symmetric-shape resonance was opposed to the asymmetric Fano resonance in the scattering spectra of individual dielectric resonators. Symmetric quasi-BICs were reported also in the non-Hermitian layered structure with the $\mathcal{PT}$ symmetry breaking serving as the source of the asymmetry inducing BIC–to–quasi-BIC transformation [13].

Another intriguing feature of BICs is their topological nature as was first reported for photonic-crystal slabs [14]. The nonzero topological charge of BICs can be used for generation of polarization singularities with subwavelength-scale metasurfaces [15] and vortex lasing from metasurfaces [16] and plasmonic lattices [17]. Switching between lasing modes with different topological charges has been realized in a plasmonic lattice with BICs by manipulating losses [18]. BICs of higher topological charge can be created by merging several low-charge BICs as shown for photonic-crystal slabs in Ref. [19]. Topological response was also observed for polaritons in the BIC-supporting patterned waveguide [20].

In this paper, we apply the topological argument to further prove the important distinction between the quasi-BICs and Fano resonances. In particular, we consider the paradigmatic BIC-supporting layered structure [21] and use non-Hermitian perturbation to generate quasi-BICs [13]. Similar metal-dielectric structures were reported to possess nontrivial topological features [22,23]. Our aim is to demonstrate with this rather simple example that the topological properties can be utilized to make a distinction between the quasi-BICs and Fano resonances. In addition, we show that our non-Hermitian structure supports lasing resonances with nonzero topological charge which can be used in vortex lasing applications.

2. Results and Discussion

We consider the three-layered structure (Figure 1) supporting a BIC due to coupling of volume plasmon excitation and Fabry-Perot resonance at the plasma frequency [21]. The structure consists of the dielectric interlayer (spacer) of thickness d_{il} and two outer layers of epsilon-near-zero (ENZ) material with the Drude permittivity and the same thicknesses $d_+ = d_-$. The need for ENZ material is due to the one-dimensional nature of our system (another option is to use anisotropic materials [24]). In addition, appearance of the BIC in this system can be associated with the effect of resonant tunneling [25], since the ENZ layers closely resemble potential barriers in quantum mechanics. Introducing loss and gain (non-Hermiticity) in a balanced way makes the system $\mathcal{PT}$-symmetric. Breaking $\mathcal{PT}$ symmetry transforms the perfect infinite-Q BIC into a quasi-BIC observed as a symmetric resonance of finite width [13]. An example of such a quasi-BIC resonance in reflection is shown in Figure 2, the permittivity of the outer layers being taken as $\varepsilon_{\pm}(\omega) = 1 \pm i\gamma - \omega_p^2/\omega^2$ in calculations. Here, ω_p is the plasma frequency and γ is the non-Hermiticity magnitude (its presence allows us to observe the resonances of finite width). As it was found out earlier in Ref. [13], the quasi-BIC resonance at the plasma frequency has a symmetric shape with the peak at the particular angle of incidence, $\theta_{BIC} = \arcsin\sqrt{\varepsilon_{il} - \left(\frac{\pi c n}{\omega_p d_{il}}\right)^2}$, that takes the value $\theta_{BIC} \approx 23.881^\circ$ at the integer number $n = 7$ and the parameters listed in the caption of Figure 1 (of course, we are not limited by those values as long as they allow us to obtain the BIC at a certain incidence angle). In contrast, the resonances at nearby frequencies have the asymmetric Fano profile clearly observed in Figure 2. Such a behavior is especially pronounced in the presence of loss and gain enhancing the reflection (as well as transmission) peak to the values exceeding the unity (in our calculations, we take $\gamma = 10^{-3}$ without loss of generality). One can expect that the subtle tuning of incidence angle can be realized in experiment using the approach analogous to that utilized for excitation of surface plasmon-polaritons [26].

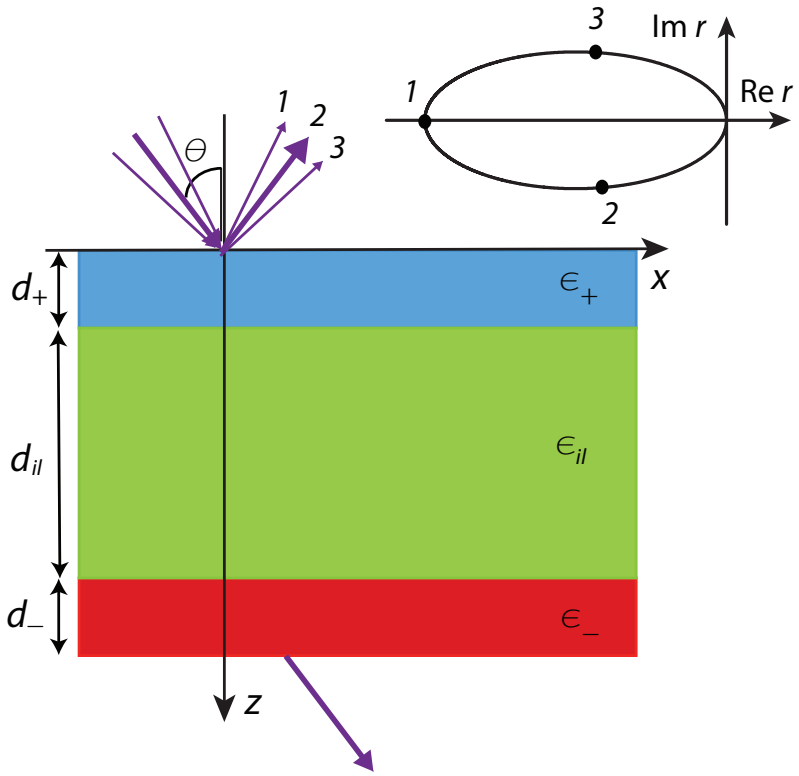

Figure 1. Schematic of a $\mathcal{PT}$-symmetric trilayer consisting of the outer layers with loss and gain ENZ media, respectively, and the dielectric spacer (or interlayer). The outer layers have the non-Hermiticity parameter γ and the thicknesses $d_\pm = \lambda_p/2\pi$ (i.e., $\omega_p d_\pm/c = 1$, where c is the speed of light). The spacer has the thickness $d_{il} = 10d_\pm$ and permittivity $\varepsilon_{il} = 5$.

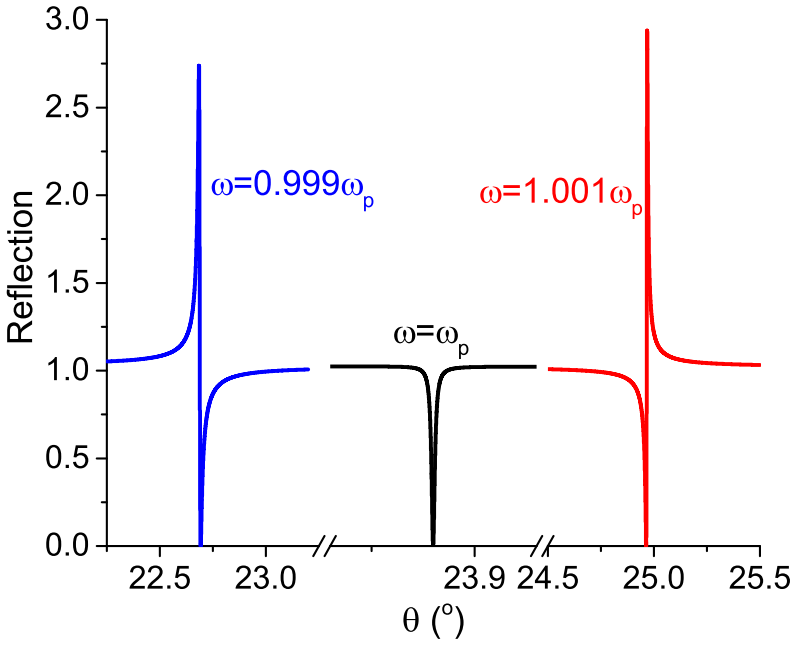

Figure 2. Dependence of reflection on the incidence angle for three different frequencies. The non-Hermiticity parameter is $\gamma = 10^{-3}$.

The reflection $R = |r|^2$ in Figure 2 is calculated using the the transfer-matrix method, where r is the amplitude reflection coefficient for TM waves [13]. The value of r is generally complex, so we can trace its trajectory in the complex plane ($\mathrm{Re}\, r$, $\mathrm{Im}\, r$) under the gradual change of the incidence angle embracing position of the resonance. To be specific, we take the range $\theta \in [\theta_-, \theta_+]$, where $\theta_\pm = \theta_c \pm \Delta\theta$ and θ_c is the central angle. The interval $\Delta\theta$ should not be too large to avoid affecting other spectral features. In our calculations, we employ $\Delta\theta = 0.5^\circ$. For the quasi-BIC in question, the central angle $\theta_c = \theta_{BIC} = 23.881^\circ$, whereas for Fano resonances, we take the central angles $\theta_c = 22.7^\circ$ and 25°, respectively. As shown in Figure 3a, the trajectory of r in the complex plane is a closed oval curve (a loop) starting from the thick dot at $r \approx -1$ that corresponds to θ_-. Positions of the curves and directions of encircling turn out to be dramatically different for the quasi-BIC and Fano resonances. As seen in the close-up plot in Figure 3b, all the curves cross the imaginary axis, but for the quasi-BIC encircling almost touches it (locally the curve is an almost vertical line). Regarding the direction of encircling, the counterclockwise encircling occurs for the quasi-BIC and the clockwise encircling does for the Fano resonance. Finally, the loop for the quasi-BIC starts and finishes exactly at the real axis, whereas the starting point of the Fano resonances is either slightly above or below the real axis. The reason for the above mentioned behavior is that the Fano lines are asymmetric with one shoulder higher than the other (see Figure 2). On the contrary, the quasi-BIC has perfectly symmetric shoulders causing symmetry of the loop and position of the starting point at $\mathrm{Im}\, r = 0$.

The closed trajectories shown in Figure 3a can be characterized with topological charges (or winding numbers) showing the number of full 2π turns of the phase obtained under encircling the trajectory. It can be calculated as follows [27],

$$W = \frac{1}{2\pi} \oint d\phi = \frac{1}{2\pi i} \oint \frac{dr}{r} = \frac{1}{2\pi i} \oint d(\ln r). \tag{1}$$

Numerically calculated winding numbers for the three trajectories presented in Figure 3a fundamentally differ from each other: $W = 1$ for the quasi-BIC and $W = 0$ for the Fano resonances. In other words, the BIC is the topologically nontrivial phenomenon, in contrast to the Fano resonances. This means that the Fano resonance at the frequency or angle close to the BIC cannot be used as a proxy to the BIC itself, as often assumed. This is an additional evidence of the deep difference between the BICs and the Fano resonances [12].

However, Figure 3b hints at some additional intriguing feature of the resonant responses discussed above. One can see that the loops in all cases cross the imaginary axis exactly at the point of $r = 0$. For general reasons connected to integration of functions with a pole in the complex plane, one would expect that there are three different situations: (i) when the pole is not embraced by the integration contour, the topological charge is zero; (ii) when the pole is embraced by the integration contour, the topological charge is an integer greater than zero; (iii) when the pole is exactly at the integration contour, the topological charge can be half-integer. Indeed, if we calculate the integral (1) in the vicinity of pole ($r = 0$), such as shown in Figure 3b, we obtain a value close to 0.5. The contribution of the remaining part of the loops makes the integral either 0 or 1. Perhaps, this feature is due to the non-Hermitian nature of our resonances, since they are connected with $\mathcal{PT}$-symmetry breaking at the exceptional point [13]. It is known that exceptional points are associated with half-integer winding numbers [28]. So, we can speculate that our quasi-BICs and Fano resonances have simultaneously features of usual singular points with integer W and exceptional points with half-integer W. This interesting possibility is worth further study.

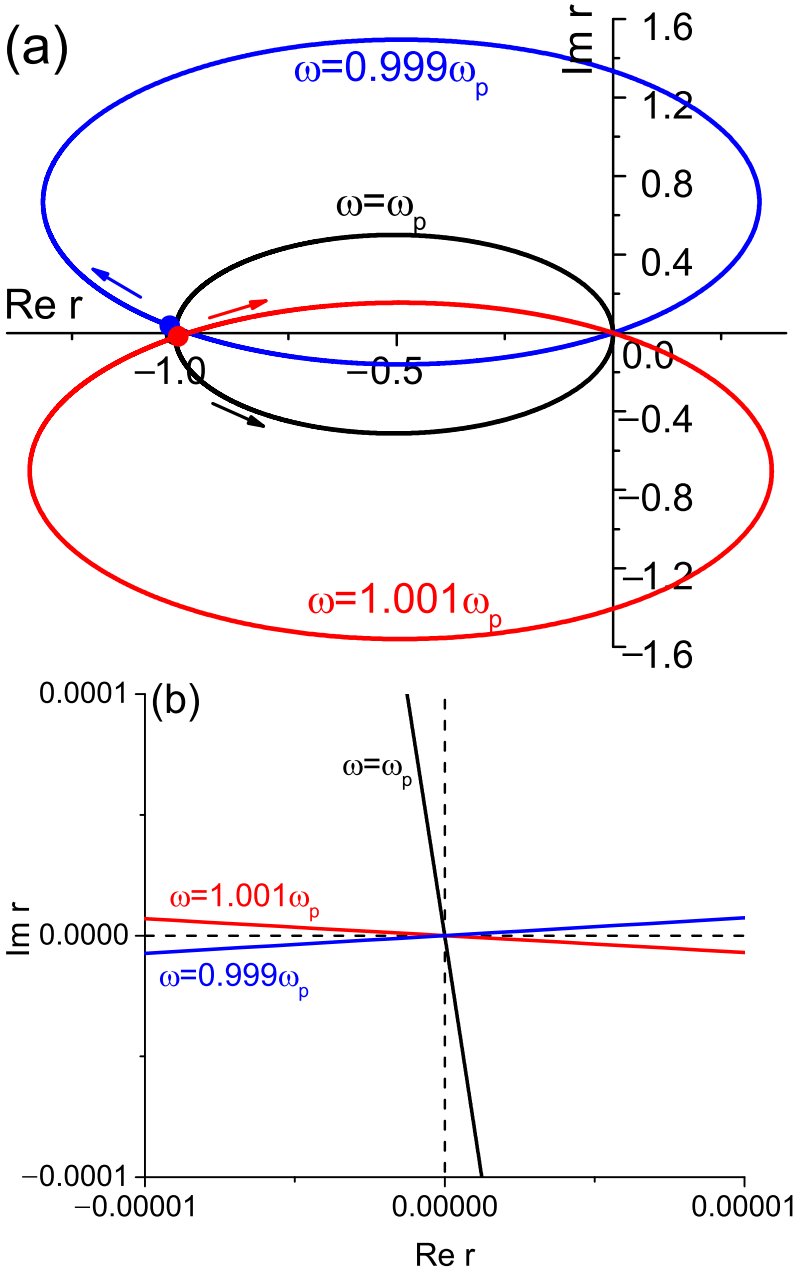

Figure 3. (**a**) The loops of reflection coefficient in the complex frequency plane corresponding to the spectra in Figure 2. The thick dots mark the starting points of the loops, the arrows show the direction of the encircling. (**b**) The close-up of the loops in the vicinity of $r = 0$. The non-Hermiticity parameter is $\gamma = 10^{-3}$.

Finally, we consider the change of the winding number, when asymmetry is introduced in the structure. Such asymmetric structures were studied recently in Refs. [29,30] and were shown to support the effect of simultaneous coherent perfect absorption (CPA) and lasing associated with the quasi-BIC resonance. Here, we consider the case of geometric asymmetry when the loss and gain layers have different thicknesses, so that $d_- = \alpha d_+$, where α is the asymmetry parameter, which shows how much thicker the gain layer is in comparison to the loss layer (with all other parameters fixed). This parameter can be changed simply by changing the thickness of gain layer. Reflection coefficients for two values of α are shown in Figure 4a,b. The case of $\alpha = 1.0112$ corresponds to the CPA-lasing condition with strong reflection amplification (Figure 4a), so that the oval trajectory of r in the complex plane has a strongly enlarged size, but still only touching the axis of imaginary

r (Figure 4c). For much larger $\alpha = 2$ (the gain layer is twice as thick as the loss layer), the reflection peak is much lower and appears at the reflection slope (Figure 4b). As a result, the trajectory gets open with the loop far from the imaginary axis as shown in Figure 4d. As our calculation shows, the winding number is still $W = 1$ in both these asymmetric cases as in the perfectly symmetric structure. One can expect that such lasing structures with nontrivial topological properties can be used for generation of structured light or optical vortexes.

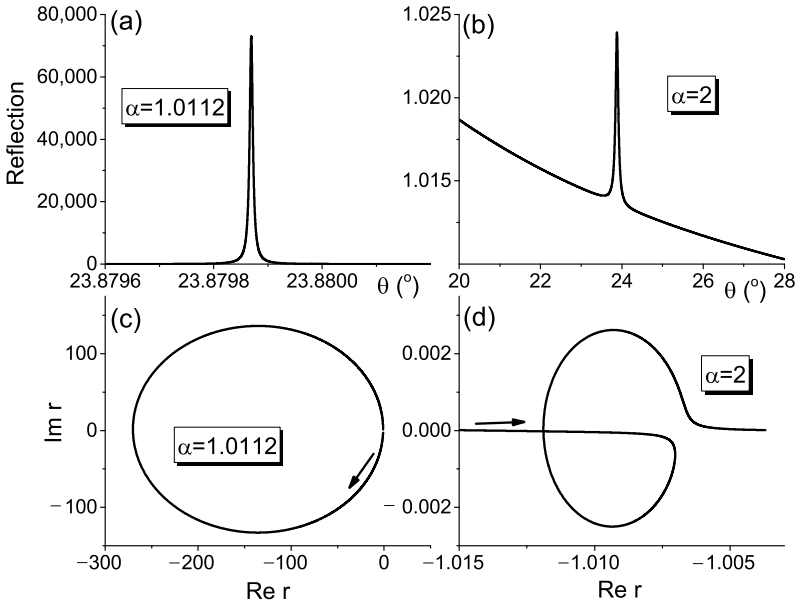

Figure 4. (**a**,**b**) Dependence of reflection on the incidence angle for the asymmetry parameters $\alpha = 1.0112$ and 2, respectively. (**c**,**d**) The corresponding loops of reflection coefficient in the complex frequency plane. The arrows show the direction of the encircling. The frequency is $\omega = \omega_p$, the non-Hermiticity parameter is $\gamma = 10^{-3}$.

3. Conclusions

To sum up, we provide a topological argument to distinguish BICs and Fano resonances. The argument is illustrated with the one-dimensional layered structure, which can be readily analyzed. In particular, we calculate the topological charge of different resonant states and show that it is zero for Fano resonances and one for BICs. The nontrivial topological nature of BICs is preserved even under strong symmetry perturbations transforming BIC into CPA-lasing point. Our finding has important implications in interpreting Fano resonances in BIC-supporting systems. Apart from this fundamental issue, it can have significance for possible applications. For example, the topological charge can play an important role in the interaction of polarized light with the BIC-supporting structures as well as for generation of structured light and vortexes in lasers governed by BICs.

We should also stress the importance of question on how universal our results are. To deal with this issue, further studies of different systems supporting BICs and Fano resonances (both Hermitian and non-Hermitian) are much needed. In particular, we have considered only a rather simple 1D structure. However, 2D and 3D ones (such as photonic-crystal slabs and metasurfaces) are very popular objects in the BIC and Fano studies. As several further examples, we mention grating-assisted ring resonators [31] and sensor devices [32,33], coupled resonators [34], mesoscale particle-based systems [35] and many more.

Author Contributions: Conceptualization, D.V.N.; methodology, D.V.N. and A.V.N.; software, D.V.N.; formal analysis, A.V.N.; investigation, D.V.N. and A.V.N.; writing—original draft preparation, D.V.N.; writing—review and editing, A.V.N.; visualization, A.V.N. All authors have read and agreed to the published version of the manuscript.

Funding: D.V.N. is grateful to the State Program for Scientific Research "Photonics and Electronics for Innovations" (Task 1.5). A.V.N. acknowledges the support of the Russian Science Foundation (Grant No. 21-12-00383) for calculation of reflection spectra.

Institutional Review Board Statement: Not applicable.

Informed Consent Statement: Not applicable.

Data Availability Statement: The data presented in this study are available on reasonable request from the corresponding author.

Conflicts of Interest: The authors declare no conflict of interest.

References

1. Krasnok, A.; Baranov, D.; Li, H.; Miri, M.-A.; Monticone, F.; Alú, A. Anomalies in light scattering. *Adv. Opt. Photon.* **2019**, *11*, 892–951.
2. Von Neumann, J.; Wigner, E. Über merkwürdige diskrete Eigenwerte. *Phys. Z.* **1929**, *30*, 465–467.
3. Stillinger, F.H.; Herrick, D.R. Bound states in the continuum. *Phys. Rev. A* **1975**, *11*, 446–454.
4. Friedrich, H.; Wintgen, D. Interfering resonances and bound states in the continuum. *Phys. Rev. A* **1985**, *32*, 3231–3242.
5. Hsu, C.W.; Zhen, B.; Stone, A.D.; Joannopoulos, J.D.; Soljačić, M. Bound states in the continuum. *Nat. Rev. Mater.* **2016**, *1*, 16048.
6. Koshelev, K.; Bogdanov, A.; Kivshar, Y. Engineering with bound states in the continuum. *Opt. Photon. News* **2020**, *31*, 38–45.
7. Azzam, S.I.; Kildishev, A.V. Photonic bound states in the continuum: From basics to applications. *Adv. Opt. Mater.* **2021**, *9*, 2001469.
8. Sadreev, A.F. Interference traps waves in open system: Bound states in the continuum. *Rep. Prog. Phys.* **2021**, *84*, 055901.
9. Koshelev, K.; Lepeshov, S.; Liu, M.; Bogdanov, A.; Kivshar, Y. Asymmetric metasurfaces with high-Q resonances governed by bound states in the continuum. *Phys. Rev. Lett.* **2018**, *121*, 193903.
10. Kupriianov, A.S.; Xu, Y.; Sayanskiy, A.; Dmitriev, V.; Kivshar, Y.S.; Tuz, V.R. Metasurface engineering through bound states in the continuum. *Phys. Rev. Appl.* **2019**, *12*, 014024.
11. Bogdanov, A.A.; Koshelev, K.L.; Kapitanova, P.V.; Rybin, M.V.; Gladyshev, S.A.; Sadrieva, Z.F.; Samusev, K.B.; Kivshar, Y.S.; Limonov, M.F. Bound states in the continuum and Fano resonances in the strong mode coupling regime. *Adv. Photon.* **2019**, *1*, 016001.
12. Melik-Gaykazyan, E.; Koshelev, K.; Choi, J.-H.; Kruk, S.S.; Bogdanov, A.; Park, H.-G.; Kivshar, Y. From Fano to quasi-BIC resonances in individual dielectric nanoantennas. *Nano Lett.* **2021**, *21*, 1765–1771.
13. Novitsky, D.V.; Shalin, A.S.; Redka, D.; Bobrovs, V.; Novitsky, A.V. Quasibound states in the continuum induced by $\mathcal{PT}$ symmetry breaking. *Phys. Rev. B* **2021**, *104*, 085126.
14. Zhen, B.; Hsu, C.W.; Lu, L.; Stone, A.D.; Soljačić, M. Topological nature of optical bound states in the continuum. *Phys. Rev. Lett.* **2014**, *113*, 257401.
15. Dang, N.H.M.; Zanotti, S.; Drouard, E.; Chevalier, C.; Trippé-Allard, G.; Amara, M.; Deleporte, E.; Ardizzone, V.; Sanvitto, D.; Andreani, L.C.; et al. Realization of polaritonic topological charge at room temperature using polariton bound states in the continuum from perovskite metasurface. *Adv. Opt. Mater.* **2022**, *10*, 2102386.
16. Huang, C.; Zhang, C.; Xiao, S.; Wang, Y.; Fan, Y.; Liu, Y.; Zhang, N.; Qu, G.; Ji, H.; Han, J.; et al. Ultrafast control of vortex microlasers. *Science* **2020**, *367*, 1018–1021.
17. Heilmann, R.; Salerno, G.; Cuerda, J.; Hakala, T.K.; Törmä, P. Quasi-BIC mode lasing in a quadrumer plasmonic lattice. *ACS Photon.* **2022**, *9*, 224–232.
18. Salerno, G.; Heilmann, R.; Arjas, K.; Aronen, K.; Martikainen, J.-P.; Törmä, P. Loss-driven topological transitions in lasing. *Phys. Rev. Lett.* **2022**, *129*, 173901.
19. Kang, M.; Mao, L.; Zhang, S.; Xiao, M.; Xu, H.; Chan, C.T. Merging bound states in the continuum by harnessing higher-order topological charges. *Light Sci. Appl.* **2022**, *11*, 228.
20. Ardizzone, V.; Riminucci, F.; Zanotti, S.; Gianfrate, A.; Efthymiou-Tsironi, M.; Suàrez-Forero, D.G.; Todisco, F.; De Giorgi, M.; Trypogeorgos, D.; Gigli, G.; et al. Polariton Bose–Einstein condensate from a bound state in the continuum. *Nature* **2022**, *605*, 447–452.
21. Monticone, F.; Doeleman, H.M.; Den Hollander, W.; Koenderink, A.F.; Alù, A. Trapping light in plain sight: Embedded photonic eigenstates in zero-index metamaterials. *Laser Photon. Rev.* **2018**, *12*, 1700220.
22. Sakotic, Z.; Krasnok, A.; Alù, A.; Jankovic, N. Topological scattering singularities and embedded eigenstates for polarization control and sensing applications. *Photon. Res.* **2021**, *9*, 1310–1323.
23. Huang, Y.; Shen, Y.; Veronis, G. Topological edge states at singular points in non-Hermitian plasmonic systems. *Photon. Res.* **2022**, *10*, 747–757.
24. Pankin, P.S.; Wu, B.-R.; Yang, J.-H.; Chen, K.-P.; Timofeev, I.V.; Sadreev, A.F. One-dimensional photonic bound states in the continuum. *Commun. Phys.* **2020**, *3*, 91.
25. Kivshar, Y. Resonant tunneling and bound states in the continuum. *Fiz. Nizk. Temp.* **2022**, *48*, 438–444.
26. Novotny, L.; Hecht, B. *Principles of Nano-Optics*; Cambrudge University Press: Cambridge, UK, 2006; pp. 387–391.

27. Ernzerhof, M.; Giguère, A.; Mayou, D. Non-Hermitian quantum mechanics and exceptional points in molecular electronics. *J. Chem. Phys.* **2020**, *152*, 244119.
28. Wang, H.; Zhang, X.; Hua, J.; Lei, D.; Lu, M.; Chen, Y. Topological physics of non-Hermitian optics and photonics: A review. *J. Opt.* **2021**, *23*, 123001.
29. Novitsky, D.V.; Canós Valero, A.; Krotov, A.; Salgals, T.; Shalin, A.S.; Novitsky, A.V. CPA-lasing associated with the quasibound states in the continuum in asymmetric non-Hermitian structures. *ACS Photon.* **2022**, *9*, 3035–3042.
30. Hlushchenko, A.V.; Novitsky, D.V.; Tuz, V.R. Trapped-mode excitation in all-dielectric metamaterials with loss and gain. *Phys. Rev. B* **2022**, *106*, 155429.
31. Brunetti, G.; Dell'Olio, F.; Conteduca, D.; Armenise, M.N.; Ciminelli, C. Comprehensive mathematical modelling of ultra-high Q grating-assisted ring resonators. *J. Opt.* **2020**, *22*, 035802.
32. Yadav, G.; Sahu, S.; Kumar, R.; Jha, R. Bound States in the Continuum Empower Subwavelength Gratings for Refractometers in Visible. *Photonics* **2022**, *9*, 292.
33. Tang, S.; Chang, C.; Zhou, P.; Zou, Y. Numerical Study on a Bound State in the Continuum Assisted Plasmonic Refractive Index Sensor. *Photonics* **2022**, *9*, 224.
34. Tu, X.; Mario, L.Y.; Mei, T. Coupled Fano resonators. *Opt. Express* **2010**, *18*, 18820–18831.
35. Minin, I.V.; Minin, O.V. Mesotronics: Some New, Unusual Optical Effects. *Photonics* **2022**, *9*, 762.